Zero applied stress rheometer

L. Bellon, L. Buisson, S. Ciliberto, and F. Vittoz
Ecole Normale Supérieure de Lyon, Laboratoire de Physique, C.N.R.S. UMR5672, 46, Allée d'Italie, 69364 Lyon Cedex 07, France

(Received 25 January 2001; accepted for publication 17 June 2002)

In order to test the fluctuation-dissipation relation on rheological properties of soft materials, we built an experiment to measure thermally excited strain in a sample and compare it to the classical response to an external stress. The rheometer is based on a cylindrical Couette geometry. We use differential interferometry to achieve better than 10^{-10} rad/$\sqrt{\text{Hz}}$ sensitivity in angular position above 0.5 Hz. The forcing method, based on electrostatic interaction in a capacitor, generates torques comparable to that of thermal noise. Experiments on a calibrated silicon oil show good agreement between response and fluctuation measurements. © *2002 American Institute of Physics.* [DOI: 10.1063/1.1499210]

I. INTRODUCTION

The measurement of any response function of a physical system is usually based on the same procedure; a *small* external forcing has to be applied to the system in order to study its response. *Small*, because we work under the fundamental hypothesis of the linear response theory.[1] The forcing of the system should not drive it to another state where its properties are different. While it is generally easy to fulfill this condition, it may become tricky in some cases. For example, systems that are very fragile or close to a critical point cannot be tested without extreme care. Likewise, systems that are still evolving must be handled with precaution; since they are not in equilibrium, any external forcing may change (delay, accelerate, etc.) their natural evolution.

For systems in equilibrium, the study of intrinsic fluctuations of one property can give an answer to that problem; in Onsager's hypothesis, these thermally excited fluctuations are governed by the same linear response functions. The fluctuation-dissipation theorem (FDT),[1] resulting from this hypothesis, allows determination of response functions from the study of fluctuations. Let us recall briefly the expression of this theorem. We consider an observable x of the system and its conjugate variable F. The response function $\chi_{xF}(f)$, at frequency f, describes the variation $\delta x(f)$ of x induced by a perturbation $\delta F(f)$ of F, that is, $\chi_{xF}(f) = \delta x(f)/\delta F(f)$. FDT relates the fluctuation spectral density of x to the response function χ_{xF} and the temperature T of the system:

$$S_x(f) = \frac{4k_BT}{\omega}\,\mathrm{Im}[\chi_{xF}(f)], \tag{1}$$

where $S_x(f) = \langle |x(f)|^2 \rangle$ is the fluctuation spectral density of x, k_B is the Boltzmann constant, $\mathrm{Im}[\chi_{xF}(f)]$ is the imaginary part of $\chi_{xF}(f)$, and $\omega = 2\pi f$. Textbook examples of FDT are Nyquist's formula relating the voltage noise to the electrical resistance and the Einstein's relation for Brownian motion relating the particle diffusion coefficient to the fluid viscosity. Therefore, the study of fluctuations can give a true zero forcing measurement of a response function. This smart technique has already been used in several experiments, to extract properties of biological, chemical, and physical systems.[2–4]

The case of out of equilibrium systems is a bit different, since the requirements of FDT are not fulfilled. However, some recent theories for glassy materials point out the interest of the study of fluctuation-dissipation ratio in these slowly aging systems.[5] Experimentally, such a measurement implies an independent determination of fluctuations and response, with a vanishing driving in the second case to avoid any modification of sample aging. Recent experiments, all focused on electrical properties of glasses, have shown the interest of such an approach.[6,7]

Our experiment was built in this context; in order to test FDT in glassy materials, we developed an original rheometer whose purpose is to measure thermally excited strain in a sample, and compare it to what can be expected from FDT. The experimental setup is based on a classic cylindric Couette rheometer configuration. To measure the angular position of the rotor, we use a differential interferometer (described in Sec. II), which permits detection of thermally excited motion. In Sec. III, we present the forcing method, based on electrostatic interaction, that we use to generate torques comparable to that of thermal noise. Section IV illustrates rheometer operation with a silicon oil, demonstrating its ability to measure response function from thermal fluctuations. We discuss in Sec. V.

II. STRAIN MEASUREMENTS: DIFFERENTIAL INTERFEROMETRY

In order to measure the infinitesimal displacements that are thermally excited in the sample, we use a differential interferometer. Originally proposed by Nomarski,[8] this technique is well suited to measure submicron displacements with better than 10^{-13} m/$\sqrt{\text{Hz}}$ sensitivity.

Figure 1 reports the optical scheme we used in our apparatus. Light emitted by a stabilized He–Ne laser (Melles Griot 05STP903) is brought to the interferometer through a polarization maintaining singlemode optical fiber. The highly

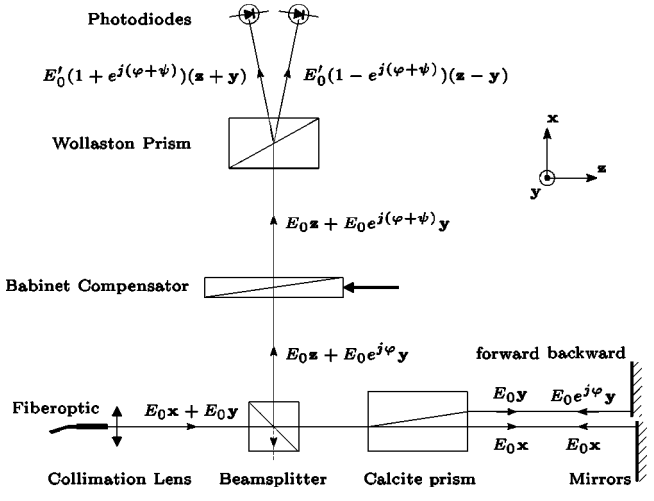

FIG. 1. Scheme of the differential interferometer. A calcite prism splits input light into two parallel beams with cross polarizations. These two beams are recombined with the same optical component after a reflection on a mirror. The phase shift φ between cross polarizations keeps track of optical path difference in the sensitive area. Analysis of this beam is made with a Wollaston prism, oriented at 45° with respect to the calcite. Contrast between intensities collected by photodiodes is a sinusoidal function of φ.

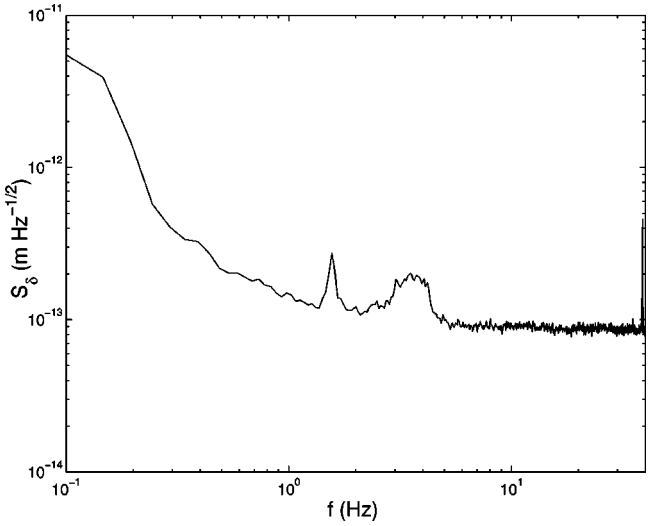

FIG. 2. Interferometer noise. With a single mirror we fix a constant difference of optical path. The output noise quantifies the resolution of the interferometer; it is better than 10^{-12} m/$\sqrt{\text{Hz}}$ above 0.6 Hz. Peaks are mechanical resonant frequencies of the apparatus, whereas the base line is due to conditioning electronics and laser phase noise.

clean divergent beam emerging from the 7-μm-diam core of the fiber is collimated with a convergent lens, and enters a calcite prism (Melles Griot 03PPD012). The polarization of the beam makes a 45° angle with the neutral axes of the crystal; thus the output consists of two parallel beams of equal intensities but with orthogonal polarizations. These two beams cross a region which is the sensitive area of the interferometer; each beam is reflected back in the calcite prism by a mirror, and the phase shift φ of one beam with respect to the other contains the information on the difference between the two optical paths $\delta L=\lambda\varphi/2\pi$.

The two beams recombine inside the calcite. The recombined beam is then sent in the analyzing branch by the beam splitter. It first crosses a Babinet compensator (Opt. J. Fichou), that adds a tunable phase ψ to the phase shift between cross polarizations. The light is further split into two beams of orthogonal polarization with a Wollaston prism (Melles Griot 03PPW003), whose neutral axes are oriented at 45° with respect to the calcite. Now interferences due to the global phase shift between the two cross polarizations are visible, and can be recorded with two low noise avalanche photodiodes (Hamamatsu SR5344).

Measured intensities are easily computed as

$$I_+=I_0[1+\cos(\varphi+\psi)],$$

$$I_-=I_0[1-\cos(\varphi+\psi)].$$

With adapted low noise analog conditioning electronics, we can measure the contrast function of these two signals:

$$C=\frac{I_+-I_-}{I_++I_-}=\cos(\varphi+\psi). \tag{2}$$

This way, we get rid of fluctuations of laser intensity, and have a direct measurement of the cosine of the total phase $\varphi+\psi$. Since variations of φ will be small in our experiments, we can choose to tune $\psi=-\pi/2$ rad, and linearize Eq. (2) to get

$$C=\sin(\varphi)\simeq\varphi=\frac{2\pi}{\lambda}\delta L. \tag{3}$$

Measurement of the contrast function C thus directly lead to that of the difference between optical path δL. This technique has been further improved to avoid linearization of Eq. (2),[9] but these developments are out of the scope of the present article. Figure 2 reports low frequency performance of the interferometer, in terms of the spectral density of δL. When the difference between optical path is fixed, output noise is lower than 10^{-12} m/$\sqrt{\text{Hz}}$ for frequencies f larger than 0.6 Hz. Residual noise is attributed to mechanical vibrations of the apparatus (pics), laser phase noise and conditioning electronic noise (base line).

Now that we have a highly efficient tool to measure variations of optical path between two parallel beams, we would like to use it to record the angular position of the rotor in the rheometer. This can be done accurately by interposing a square prism in the light path, and using a single mirror, as shown in Fig. 3(a). When the two beams enter the cube on both sides of a diagonal, the variation of δL is just proportional to that of the angular position θ of the prism; as shown in Fig. 3(b), a linear approximation is excellent in all the range accessible in θ:

$$\delta L=L_0\theta. \tag{4}$$

For our experimental conditions, we compute $L_0=20$ mm/rad with a 30° range available in theta. Thus using this deflection technique the contrast is proportional to θ. Specifically, inserting Eq. (4) in Eq. (3):

$$C=\frac{2\pi}{\lambda}L_0\theta=A\theta \tag{5}$$

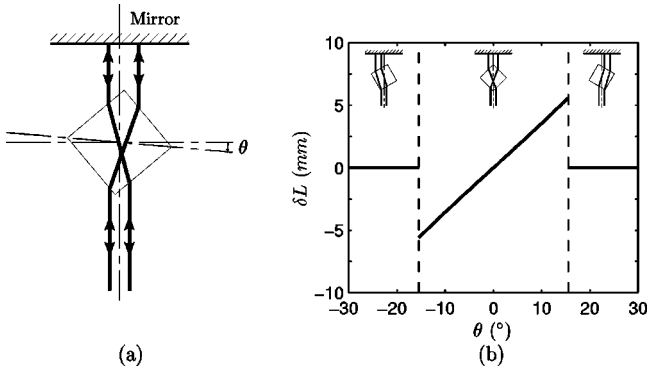

FIG. 3. (a) When the beams go through a square prism, the optical path difference δL is modified. It is a function of the angle θ between the prism and optical axis. (b) We plot $\delta L(\theta)$, computed for a BK7 ($n=1.5$) prism with a 15 mm side. This function is almost linear for $|\theta|<15°$; it is fitted by $\delta L = L_0 \theta$ with $L_0 = 20$ mm/rad.

with $A = 2.09\ 10^5$ rad^{-1}. Advantages of this deflection technique are the following: insensitivity to any translation of the prism to rotation around the optical axis, no pointing error due to any displacement, and easy positioning. Moreover, sensitivity to rotations around the second horizontal axis are second order terms in the optical path expression. Therefore, this deflection technique together with the differential interferometer allows 10^{-11} rad/$\sqrt{\text{Hz}}$ sensitivity for the detection of rotation around a vertical axis only.

III. RHEOMETER SETUP AND LOW STRESS GENERATION

Figure 4 illustrates the rheometer setup. A rotor is suspended by two steel wires in a cell of radius $R_C = 7$ mm. The rotor, which is made of poly-vinyl chloride (PVC) to reduce its inertial moment J, has a radius $R_R = 6$ mm and a height $H_R = 30$ mm. The sample fills the 1 mm gap between the rotor and the stainless steel cell. Suspension steel wires have a diameter of 0.2 mm and are tightened to ensure correct centering of the cylindric Couette setup, and to fix the resonant frequency of the torsion pendulum in the middle of the measuring frequency range. In order to remain within the linear range of the interferometer, the displacements due to the forcing technique must remain very small, thus the torque acting on the rotor too. We chose to use electrostatic interaction to achieve this goal, as shown in Fig. 4: two small metallic cylinders (labeled A_1 and A_2), fixed on the rotor, are set in correspondence with two others (labeled B_1 and B_2), fixed on the external cell. Each pair of cylinders (A_1-B_1 and A_2-B_2) constitutes a capacitor. Applying a voltage $\delta v = v_B - v_A$ between them creates an attractive force F_i ($i=1,2$) between corresponding cylinders. Respecting the symmetry around the vertical rotation axis, the total force is zero and we end up with a torque Γ acting on the rotor, tending to align all the cylinders in the same plane. Cylinders to apply torque have a 3 mm diameter for a 10 mm height and their distance is about 2 mm. The resulting capacitance is of the order of the pF. Useful driving is achieved when δv is a white noise with a peak amplitude of about 100 V.

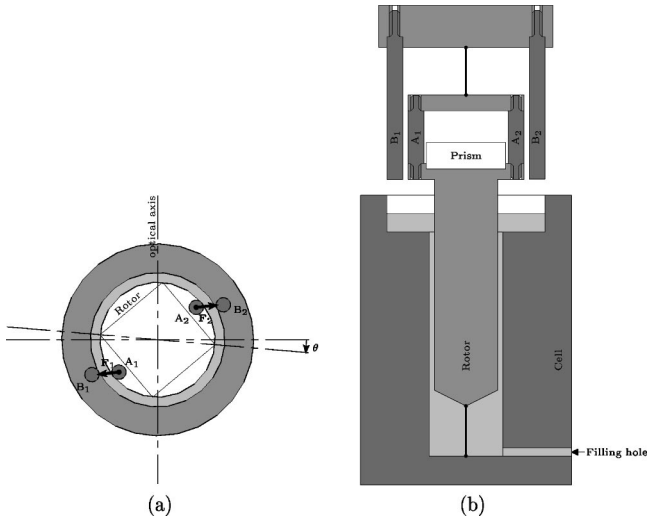

FIG. 4. Rheometer setup, top (a) and side (b) view. The rotor is suspended in the cylindrical cell with two steel wires; it behaves as a torsion pendulum whose damping coefficient can be linked to the sample rheological properties. To apply a torque, we use electrostatic interaction between cylinders $A_{1,2}$, fixed to the rotor, and $B_{1,2}$, attached to the outside cell. When submitted to a voltage $\delta v = v_B - v_A$, the two capacitors A_1-B_1 and A_2-B_2 create a δv^2 dependent torque tending to align all cylinders in a single plane.

Knowing the value of the torque as a function of the applied voltage and angular position is far too complicated to be trusted, therefore, we cannot directly access the torque value. But we know that Γ, created by electrostatic interaction, is a quadratic function of the driving voltage δv, that is,

$$\Gamma = B\,\delta v^2, \tag{6}$$

where B is a proportionality constant, which depends on the precise positioning of the cylinders. It can be determined by the inertial calibration procedure described in the next paragraph. This electrostatic stress method allows us to apply extremely tiny torque to the rotor, of order of magnitude 10^{-12} N m/$\sqrt{\text{Hz}}$.

To study the rheological behavior of the sample, we have to measure the response of the rotor to an external forcing, i.e., the response function $\chi_{\theta\Gamma} = \delta\theta(f)/\Gamma(f)$ where $\delta\theta(f)$ and $\Gamma(f)$ are, respectively, the amplitudes at frequency f of the angular position variation $\delta\theta$ and of the applied torque Γ. For small displacements, $\delta\theta$ is simply proportional to the output of the interferometer, the contrast C. Being Γ linear in δv^2, then in Fourier space $\chi_{\theta\Gamma}$ is just proportional to the transfer function χ_{Cv^2}. Specifically, using Eqs. (5) and (6):

$$\chi_{\theta\Gamma} = \frac{\delta\theta(f)}{\Gamma(f)} = \frac{A}{B}\frac{C(f)}{\Delta(f)} = \frac{A}{B}\chi_{Cv^2}, \tag{7}$$

where $\Delta(f)$ is the amplitude at frequency f of the Fourier transform of δv^2. The proportionality constant $P_c = A/B$ in Eq. (7) can be found using an inertial calibration of the measurement.

To illustrate this method, we consider that the cell is filled with a fluid of viscosity η and density ρ and that the rotor is subjected to an oscillating external torque of amplitude $\Gamma(f)$ and pulsation $\omega = 2\pi f$. In such a case the equation of motion of the rotor in Fourier space is

$$-J\ \omega^2\ \delta\theta(f) - i\ \alpha\ \omega\delta\theta(f) + k\ \delta\theta(f) = \Gamma(f), \tag{8}$$

where J is the rotor inertia moment, k the steel wires stiffness, and α is a geometric factor which depends on the size of the rotor and of the gap between the cell and the rotor. For our geometry $\alpha = 4\pi \quad H_R/(1/R_R^2 - 1/R_C^2) = (5 \pm 0.5)\ 10^{-5}\ \mathrm{m}^3$, within the approximation that the velocity profile of the fluid inside the gap between the rotor and the cell is linear, that is $(R_C - R_R)^2 < \eta/(2\pi\ f\ \rho)$. Equation (8) directly leads to the expression of the response function of this torsion pendulum

$$\chi_{\theta\Gamma} = \frac{\delta\theta(f)}{\Gamma(f)} = \frac{1}{(k - J\omega^2) - i\alpha\ \ \eta\ \ \omega}. \tag{9}$$

From Eq. (9) we see that $\mathrm{Re}(1/\chi_{\theta\Gamma}) = (k - J\omega^2)$ is a parabola whose quadratic coefficient is J. The rotor inertia moment J, being known with good accuracy, can be used to calibrate the measurement. From Eq. (7) we find that

$$\mathrm{Re}\left(\frac{1}{\chi_{Cv^2}}\right) = P_c\ \ (k - J\omega^2). \tag{10}$$

To determine P_c we have just to fit the real part of the inverse of the transfer function $1/[\chi_{Cv^2}(f)]$ with a parabola. The coefficient of the quadratic term is just the product of $P_c\ J$.

Thus P_c is determined with good accuracy from this parabolic fit. The inertial calibration technique allows a precise reading of the applied torque, and a complete determination of the response function $\chi_{\theta\Gamma}$. After calibration, the response function can of course be generalized for any fluid of complex shear modulus $G = G_1 - i\ \ G_2$, specifically,

$$\chi_{\theta\Gamma} = \frac{\delta\theta(f)}{\Gamma(f)} = \frac{1}{(\alpha G_1 + k - J\omega^2) - i\alpha G_2}. \tag{11}$$

IV. RHEOMETER OPERATION

To excite the rheometer we used a white noise source for δv. Simultaneous acquisition of C and δv is done by a computer via a 16 bits data acquisition system. The computer calculates δv^2 and the response function χ_{Cv^2}.

To test the performance of the rheometer, we study a silicon oil whose viscosity, measured with an industrial rheometer (HAAKE, SR100), is $G_1 \simeq 0$ and $\eta = (3.3 \pm 0.1)\,\mathrm{Pa\,s}$ at $\omega = 0$. In Fig. 5, we plot as a function of frequency, the real and imaginary part of the inverse of the response function of our rheometer, $1/\chi_{\theta\Gamma}$. As expected from Eqs. (9) and (10), the real part is a parabola centered on $f = 0$ Hz. The fit of this parabola allows us to determine P_C and k. Once P_c is known, from the linear fit of the imaginary part (for $f \to 0$), we can access the value of the viscosity; for a Newtonian liquid, the slope is the viscosity up to the known geometrical factor α. We measure $\eta = (3.2 \pm 0.3)\,\mathrm{Pa\,s}$, in agreement with the other measurement. The main source of uncertainty in this determination is that for the geometrical factor α, we cannot ensure better than 10% centering of the rotor with our current experimental setup. We notice a deviation to the linear behavior for $f > 20$ Hz; it is due to the non-Newtonian behavior of this silicon oil at high frequencies.

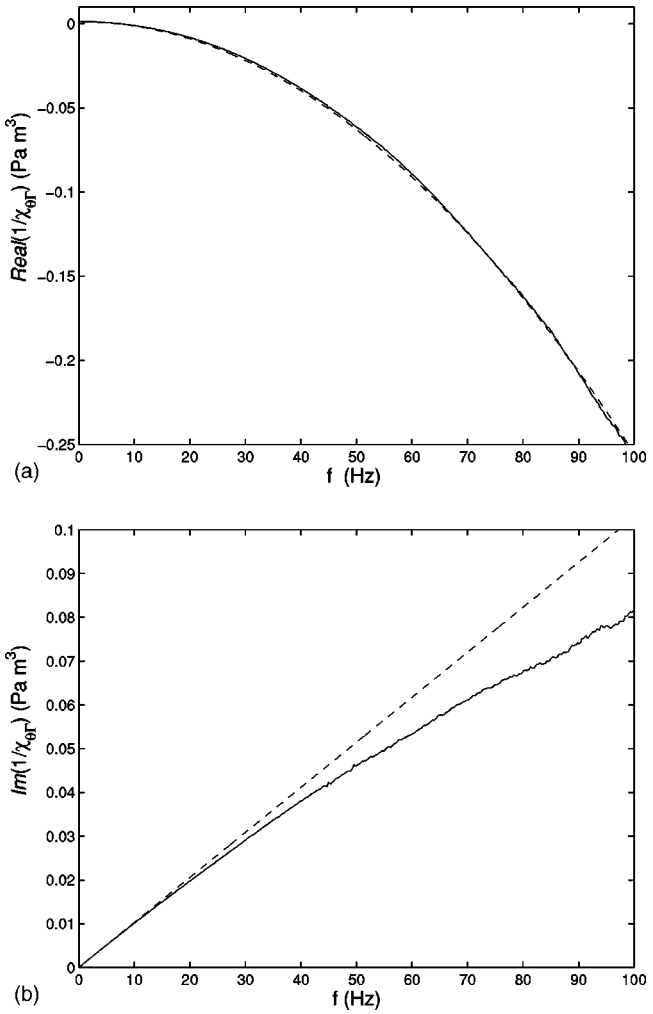

FIG. 5. Response of the rheometer to a white noise excitation. The real (a) and imaginary (b) part of $1/\chi_{\theta\Gamma}$ are plotted as a function of frequency. The rheometer is filled with a viscous oil with $\eta = 3.3$ Pa s. The dashed curve in (a) corresponds to a quadratic fit of the data, and allows inertial calibration of the measurement (see the text for details). The dashed line in (b) is a linear fit of low frequency data, it is consistent with a Newtonian behavior of the fluid and leads to a viscosity of $\eta = 3.2$ Pa s $\pm 10\%$.

This measurement corresponds to a classic rheological experiment, except for the tiny values of stress and strain applied to the material: the rms value of the shear applied is less than $10^{-4}\ \mathrm{s}^{-1}$ with a rms displacement of about 4 nm. But we can even perform a true zero applied stress determination of viscosity with this experimental setup. Indeed, let us apply FDT to the rheometer, that is rewrite Eq. (1) for coupled variables θ and Γ; when no external forcing is applied, the angular position fluctuation spectrum S_θ is given by

$$S_\theta = \frac{4k_BT}{\omega}\mathrm{Im}(\chi_{\theta\Gamma}). \tag{12}$$

Thus measuring thermal noise of the rotor angular position gives a determination of the imaginary part of $\chi_{\theta\Gamma}$, with true zero forcing. In Fig. 6 we plot the measured noise spectrum and that computed using Eq. (12) and the previously determined values of $\chi_{\theta\Gamma}$. The agreement with the prediction of FDT is good between 0.2 and 100 Hz (the peaks above 15

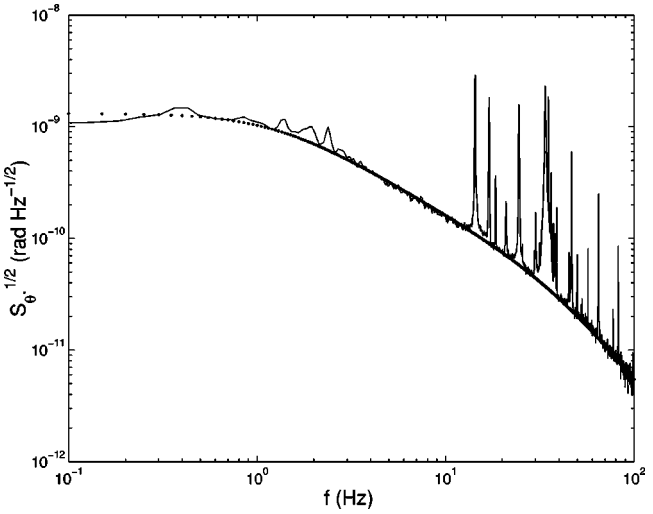

FIG. 6. Spectrum of the thermal fluctuations of θ. The rheometer is filled with the same oil used to measure the response reported in Fig. 5. The continuous line is the result of the measurement whereas the dotted line is computed-inserting into Eq. (12), the measured response of the rheometer and $T=300$ K.

Hz are due to mechanical vibrations, which are amplified by the rheometer). This agreement shows that FDT can be used to determine viscosity of a liquid, without applying any shear to it.

Indeed from the best fit of noise spectrum using Eq. (12) one can measure the viscosity which is the only unknown of Eq. (12). From this best fit we get $\eta=(3.05\pm0.3)$ Pa s which is in good agreement with the value measured directly.

V. DISCUSSION

In this article, we described a rheological experiment based on a classic cylindrical Couette setup. The use of a differential interferometer combined to a deflection technique allows us to measure the angular position with a sensitivity better than 10^{-10} rad/$\sqrt{\text{Hz}}$. Extremely low shear can be applied to the sample; using electrostatic interaction in a capacitor, we can apply torques as small as 10^{-12} N m to the rotor. An inertial calibration of the measurement allows us complete determination of the response function of the rheometer.

This rheometer can be used in two different ways:

(i) Classical rheological measurement. Applying a small external driving, we deduce from the measurement of $\chi_{\theta\Gamma}$ and Eq. (11) the value of G.

(ii) Noise measurement. Without any external forcing, we record angular position noise S_θ. If the sample is at equilibrium, FDT is valid and Eqs. (11) and (12) allow us to determine G. [From Eq. (12) only the imaginary part of $\chi_{\theta\Gamma}$ can be determined, but the real part can be deduced via Kramers–Kronig relations.]

This second procedure provides a new tool to investigate rheological properties of a media. When used alone, it provides a true zero stress rheological measurement, that, for example, can be useful for highly fragile materials. When compared to the classical measurements, it tests the validity of linear response hypothesis; if the two measurements disagree, the sample is out of equilibrium. This can be due either to intrinsic process in the material (e.g., aging, chemical reactions, etc.) or to the external forcing applied in the classical measurement.

This rheological experiment was built in order to test FDT in aging materials, preliminary results of this application can be found in Ref. 10. Based on a cylindric Couette setup, this technique can certainly be extended to other materials or configurations, and may find useful applications in various research domains.

ACKNOWLEDGMENTS

The authors acknowledge useful discussions with J. F. Palierne and H. Gayvallet. We thank P. Metz for technical support. This work has been partially supported by the Région Rhône-Alpes contract ''Program Thématique: Vieillissement des matériaux amorphes.''

[1] S. R. de Groot and P. Mazur, *Non-Equilibrium Thermodynamics* (Dover, New York, 1984).
[2] F. Gittes, B. Schnurr, P. D. Olmsted, F. C. MacKintosh, and C. F. Schmidt, Macromolecules **30**, 7781 (1997).
[3] F. Gittes, B. Schnurr, P. D. Olmsted, F. C. MacKintosh, and C. F. Schmidt, Phys. Rev. Lett. **79**, 3286 (1997).
[4] *Light Scattering by Liquid Surfaces and Complementary Techniques*, edited by D. Langevin (Marcel Dekker, New York, 1992).
[5] J. P. Bouchaud, L. F. Cugliandolo, J. Kurchan, and M. Mézard, in *Spin Glasses and Random Fields*, edited by A. P. Young (World Scientific, Singapore, 1998); also in cond-mat/9702070.
[6] T. S. Grigera and N. Israeloff, Phys. Rev. Lett. **83**, 5038 (1999).
[7] L. Bellon, S. Ciliberto, and C. Laroche, Europhys. Lett. **53**, 511 (2001).
[8] G. Nomarski, J. Phys. Radium **16**, 9S (1995).
[9] L. Bellon, S. Ciliberto, H. Boubaker, and L. Guyon, Opt. Commun. **207**, 49 (2002).
[10] L. Bellon and S. Ciliberto, Physica D (to be published); also in cond-mat/0201224.